

1 Zonal Wind Plots

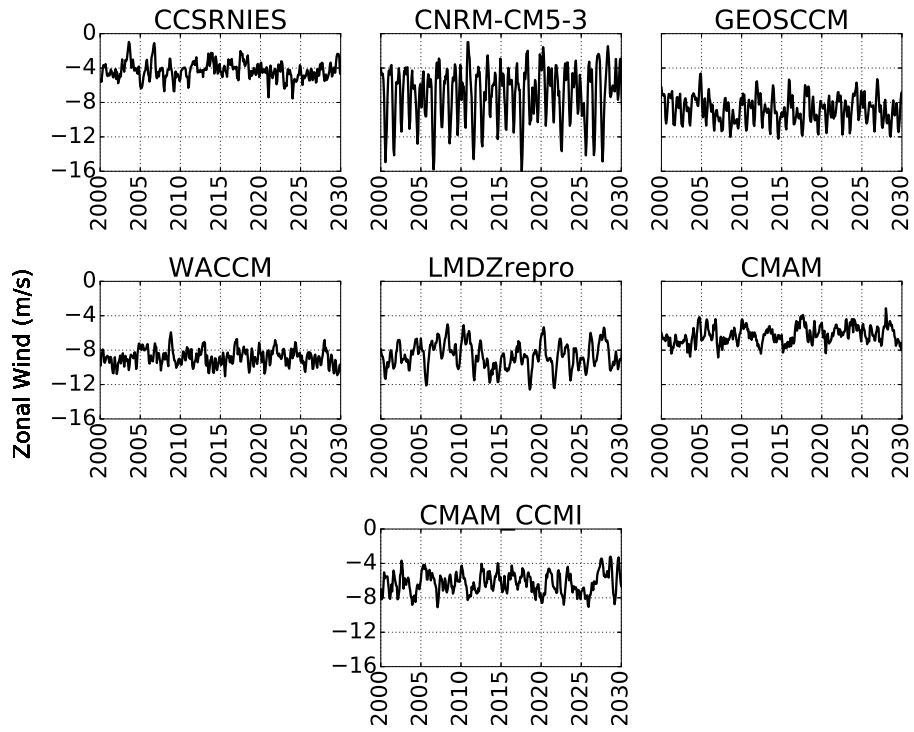


Figure 1: Time series of 50-hPa equatorial zonal winds (averaged between -5° S and 5° N) produced by CCMs not simulating a QBO.

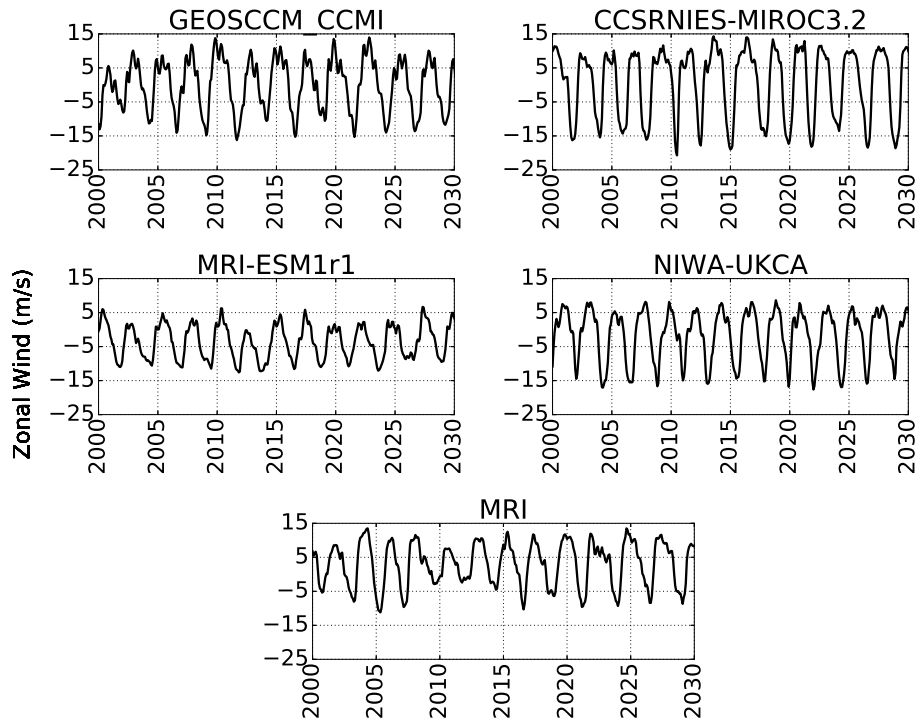


Figure 2: Time series of 50-hPa equatorial zonal winds (averaged between -5° S and 5° N) produced by CCMs simulating a QBO.

2 Regression Plots

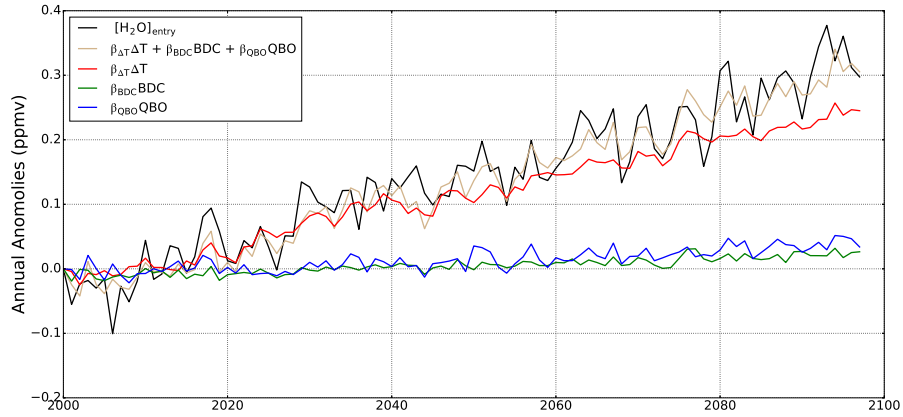


Figure 3: Time series of annual-averaged anomalies of $[H_2O]_{entry}$ from the CCSRNIES (black), and its reconstruction using a multivariate linear regression (brown). The red, green, and blue lines are the ΔT , BDC, and QBO terms from the regression, respectively.

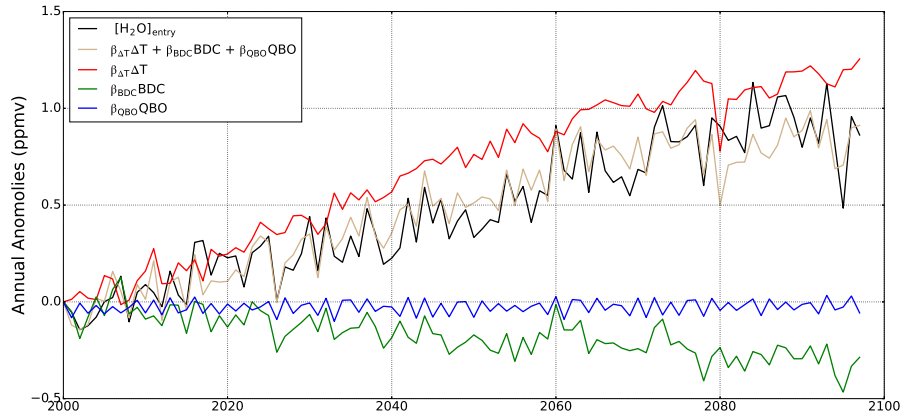


Figure 4: Time series of annual-averaged anomalies of $[H_2O]_{entry}$ from the CCSRNIES-MIROC3.2 (black), and its reconstruction using a multivariate linear regression (brown). The red, green, and blue lines are the ΔT , BDC, and QBO terms from the regression, respectively.

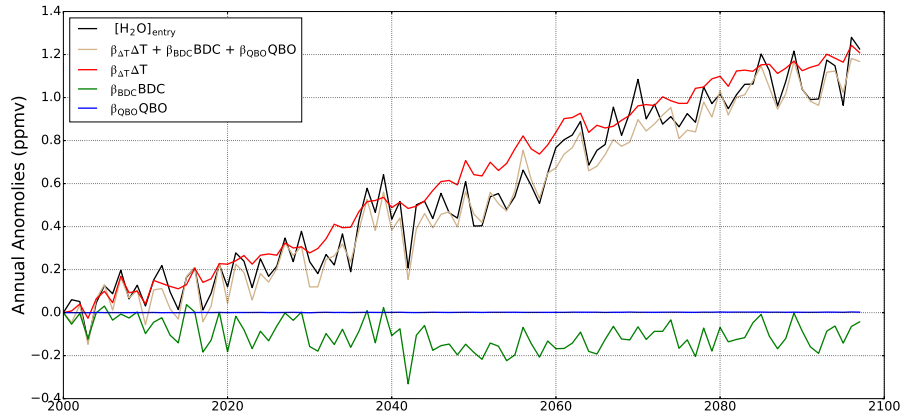


Figure 5: Time series of annual-averaged anomalies of $[H_2O]_{entry}$ from the CMAM (black), and its reconstruction using a multivariate linear regression (brown). The red, green, and blue lines are the ΔT , BDC, and QBO terms from the regression, respectively.

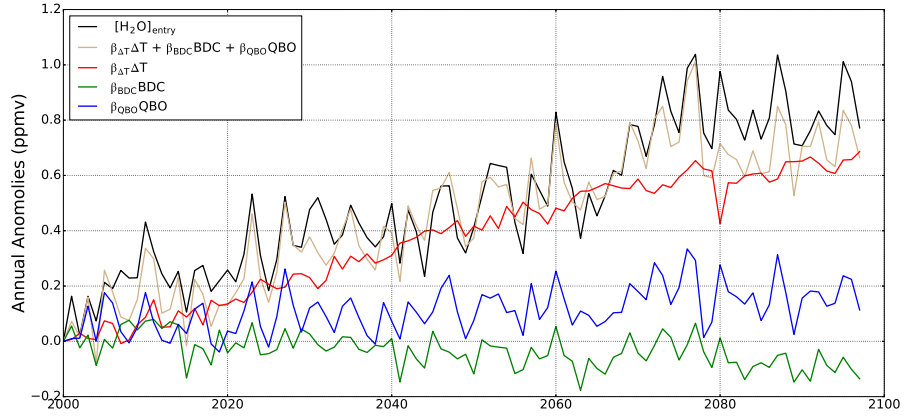


Figure 6: Time series of annual-averaged anomalies of $[H_2O]_{entry}$ from the CMAM-CCMI (black), and its reconstruction using a multivariate linear regression (brown). The red, green, and blue lines are the ΔT , BDC, and QBO terms from the regression, respectively.

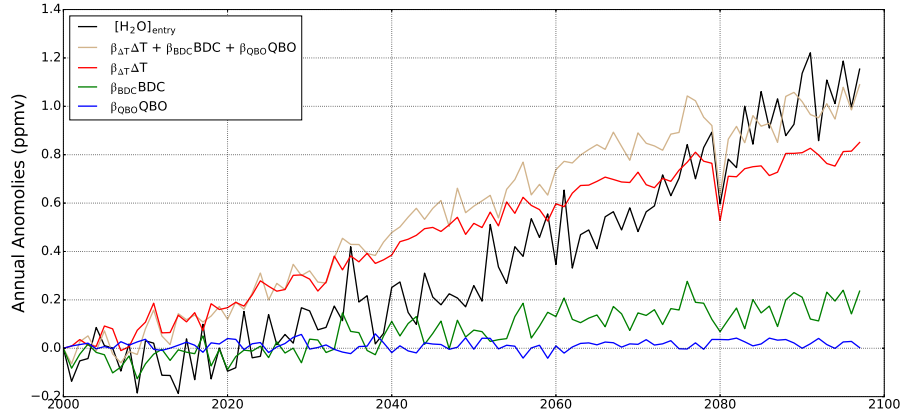


Figure 7: Time series of annual-averaged anomalies of $[H_2O]_{entry}$ from the CNRM-CM5-3 (black), and its reconstruction using a multivariate linear regression (brown). The red, green, and blue lines are the ΔT , BDC, and QBO terms from the regression, respectively.

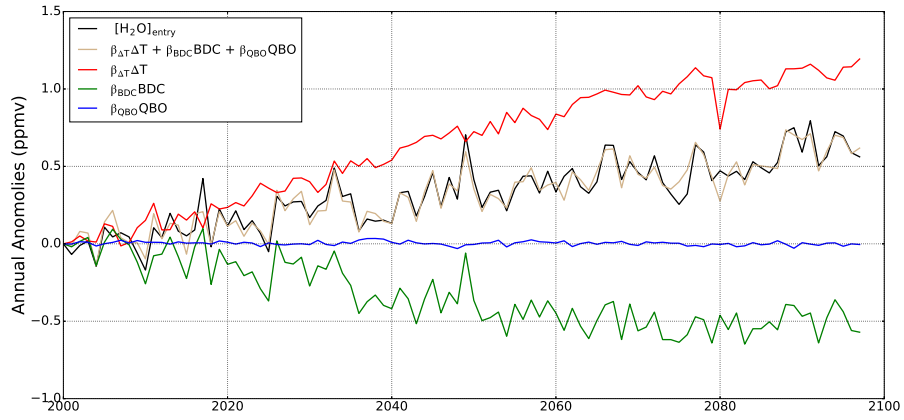


Figure 8: Time series of annual-averaged anomalies of $[H_2O]_{entry}$ from the GEOSCCM (black), and its reconstruction using a multivariate linear regression (brown). The red, green, and blue lines are the ΔT , BDC, and QBO terms from the regression, respectively.

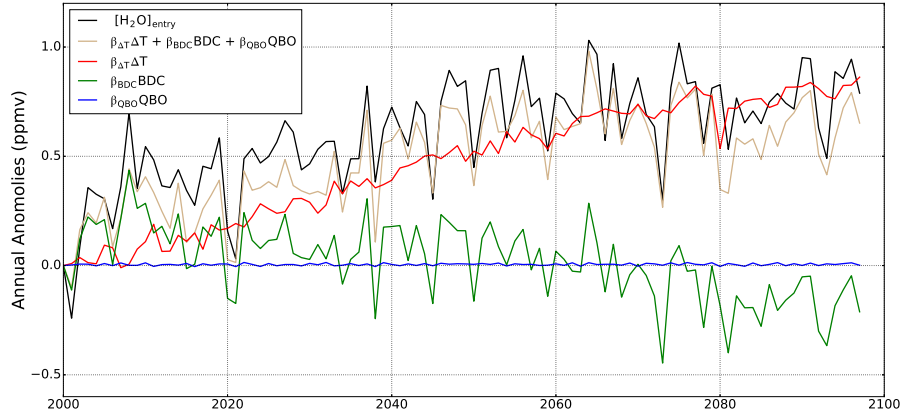


Figure 9: Time series of annual-averaged anomalies of $[H_2O]_{entry}$ from the GEOSCCM-CCMI (black), and its reconstruction using a multivariate linear regression (brown). The red, green, and blue lines are the ΔT , BDC, and QBO terms from the regression, respectively.

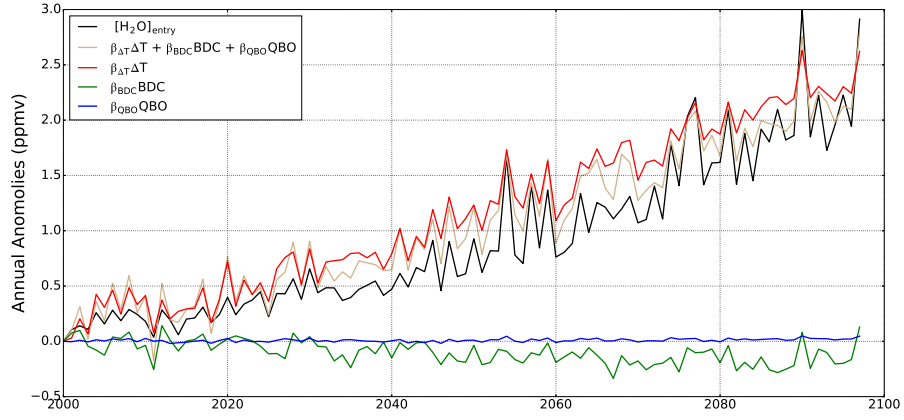


Figure 10: Time series of annual-averaged anomalies of $[H_2O]_{entry}$ from the LMDZrepro (black), and its reconstruction using a multivariate linear regression (brown). The red, green, and blue lines are the ΔT , BDC, and QBO terms from the regression, respectively.

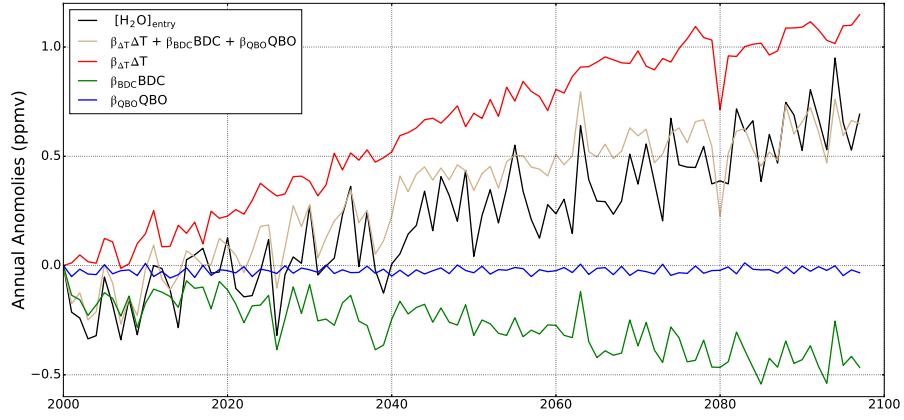


Figure 11: Time series of annual-averaged anomalies of $[H_2O]_{entry}$ from the MRI-ESM1r1 (black), and its reconstruction using a multivariate linear regression (brown). The red, green, and blue lines are the ΔT , BDC, and QBO terms from the regression, respectively.

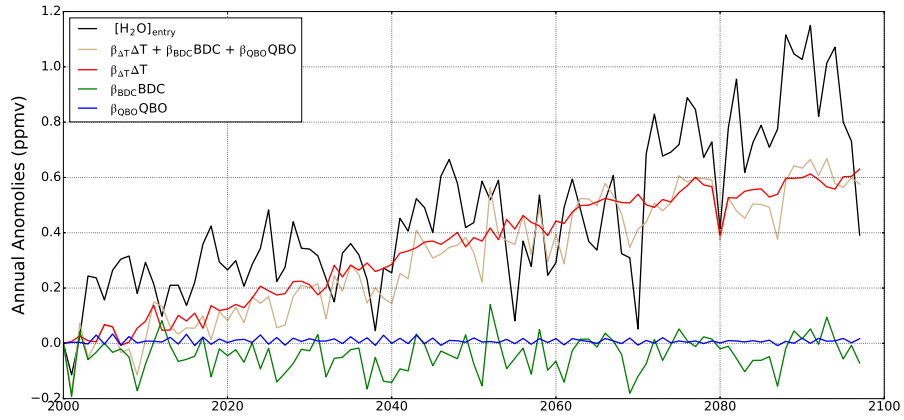


Figure 12: Time series of annual-averaged anomalies of $[H_2O]_{entry}$ from the NIWA-UKCA (black), and its reconstruction using a multivariate linear regression (brown). The red, green, and blue lines are the ΔT , BDC, and QBO terms from the regression, respectively.

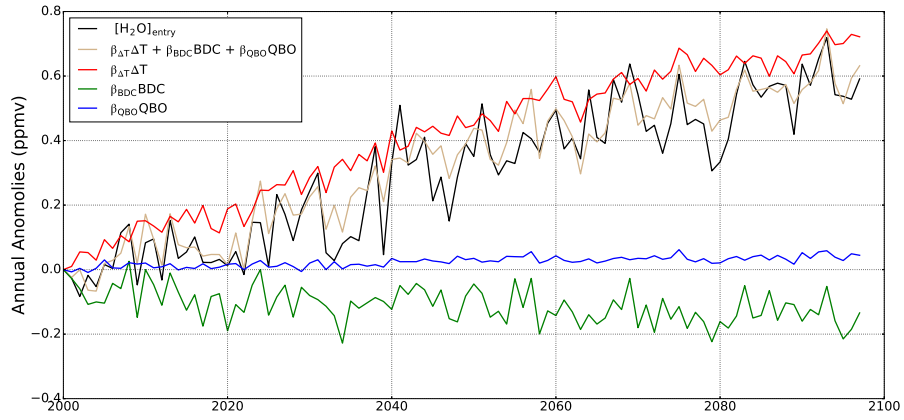


Figure 13: Time series of annual-averaged anomalies of $[H_2O]_{entry}$ from the WACCM (black), and its reconstruction using a multivariate linear regression (brown). The red, green, and blue lines are the ΔT , BDC, and QBO terms from the regression, respectively.